Electronic Supplementary Material (ESI) for Journal of Materials Chemistry A.

Electronic Supplementary Information

Sn-doped thioantimonate superionic conductors with high air stability and enhanced Li-ion conduction for all-solid-state lithium batteries

Zhihui Ma[a], Jie Shi[a], Di Wu[a], Dishuang Chen[a], Shuai Shang[a], Xuanhui Qu[a], Ping Li*[ab]

[a] *Beijing Advanced Innovation Center for Materials Genome Engineering, Institute for Advanced Materials and Technology, University of Science and Technology Beijing, Beijing 100083, PR China*

[b] *Shanxi Beike Qiantong Energy Storage Science and Technology Research Institute Co. Ltd., Gaoping 048400, PR China*

* Corresponding author.

E-mail address: ustbliping@126.com.

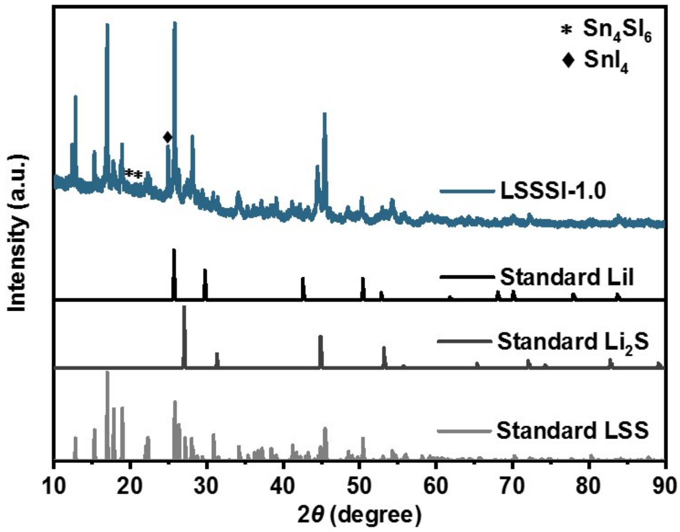

Fig. S1. XRD pattern of the synthesized LSSSI-1.0 material.

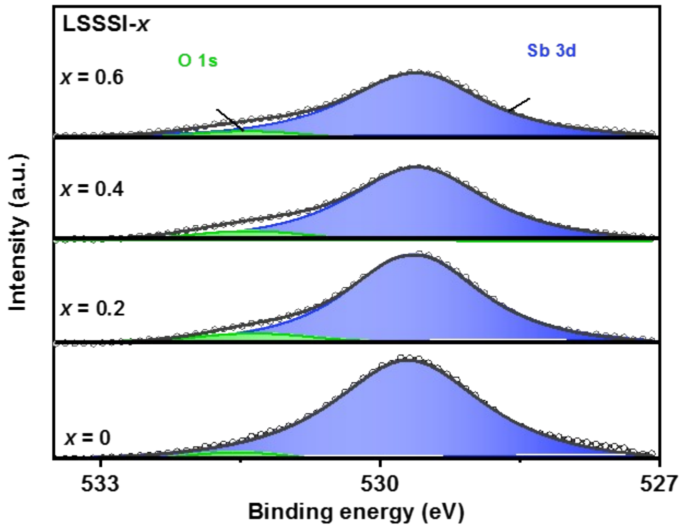

Fig. S2. Sb 3d XPS spectra for LSSSI-*x* ($0.0 \le x \le 0.6$) electrolytes. The minor peak at 531.6 eV (green) is attributed to antimony oxide caused by surface contaminations.[1-3]

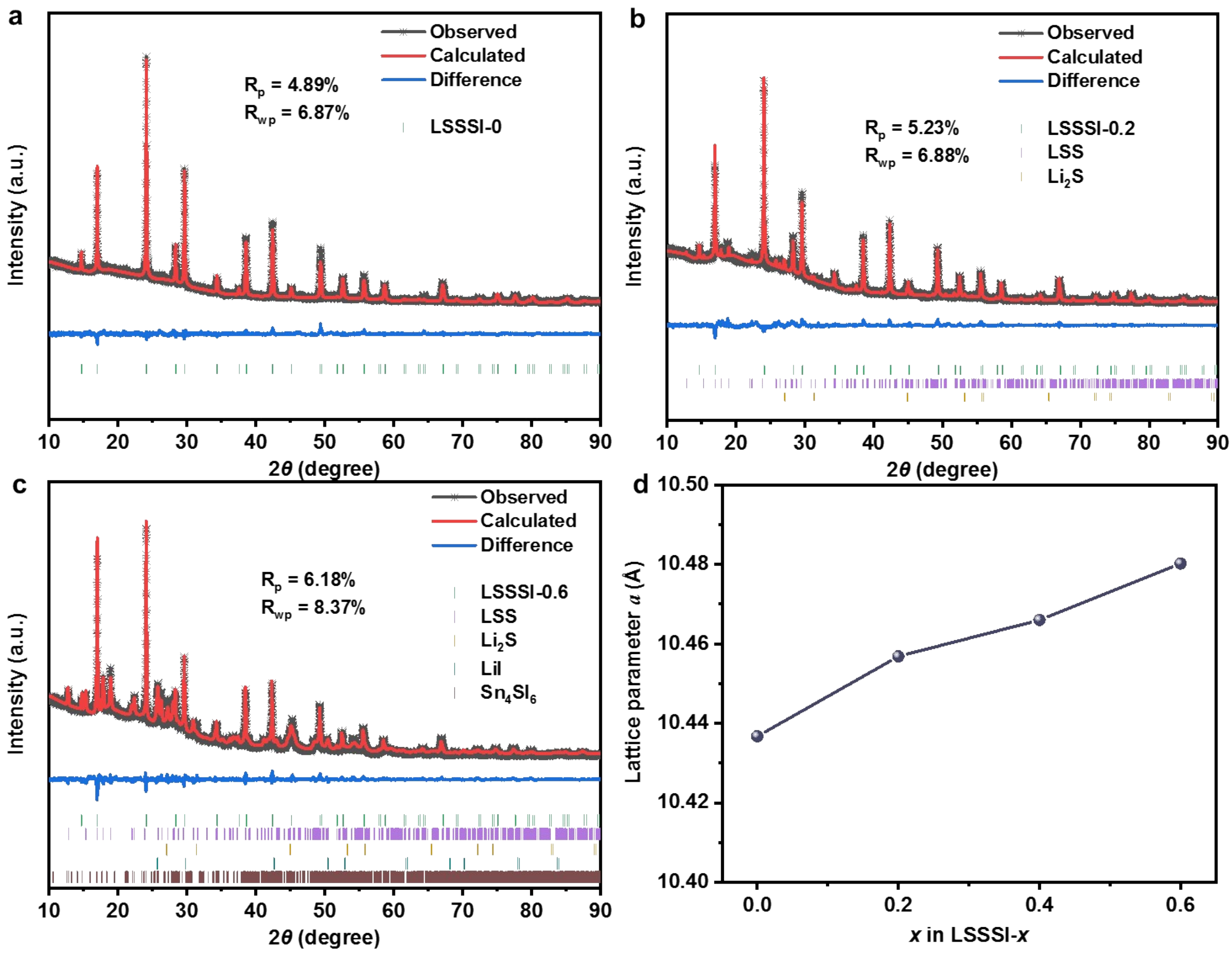

Fig. S3. Rietveld refinements of (a) LSSSI-0, (b) LSSSI-0.2 and (c) LSSSI-0.6 materials. (d) Compositional dependence of the lattice parameter for LSSSI-*x*.

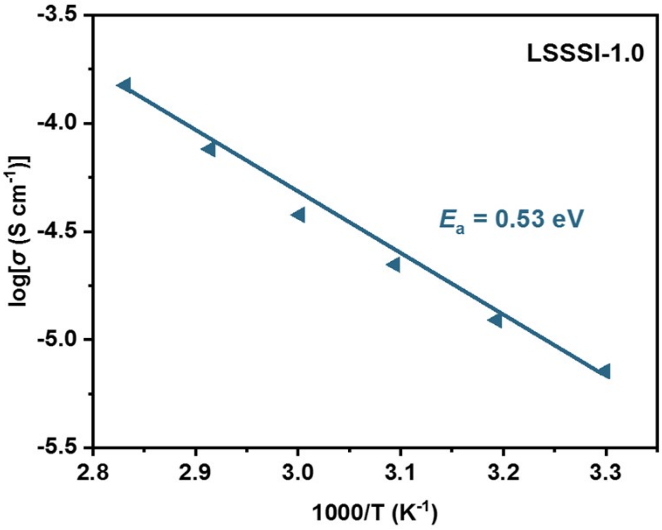

Fig. S4. Arrhenius profile of LSSSI-1.0 electrolyte.

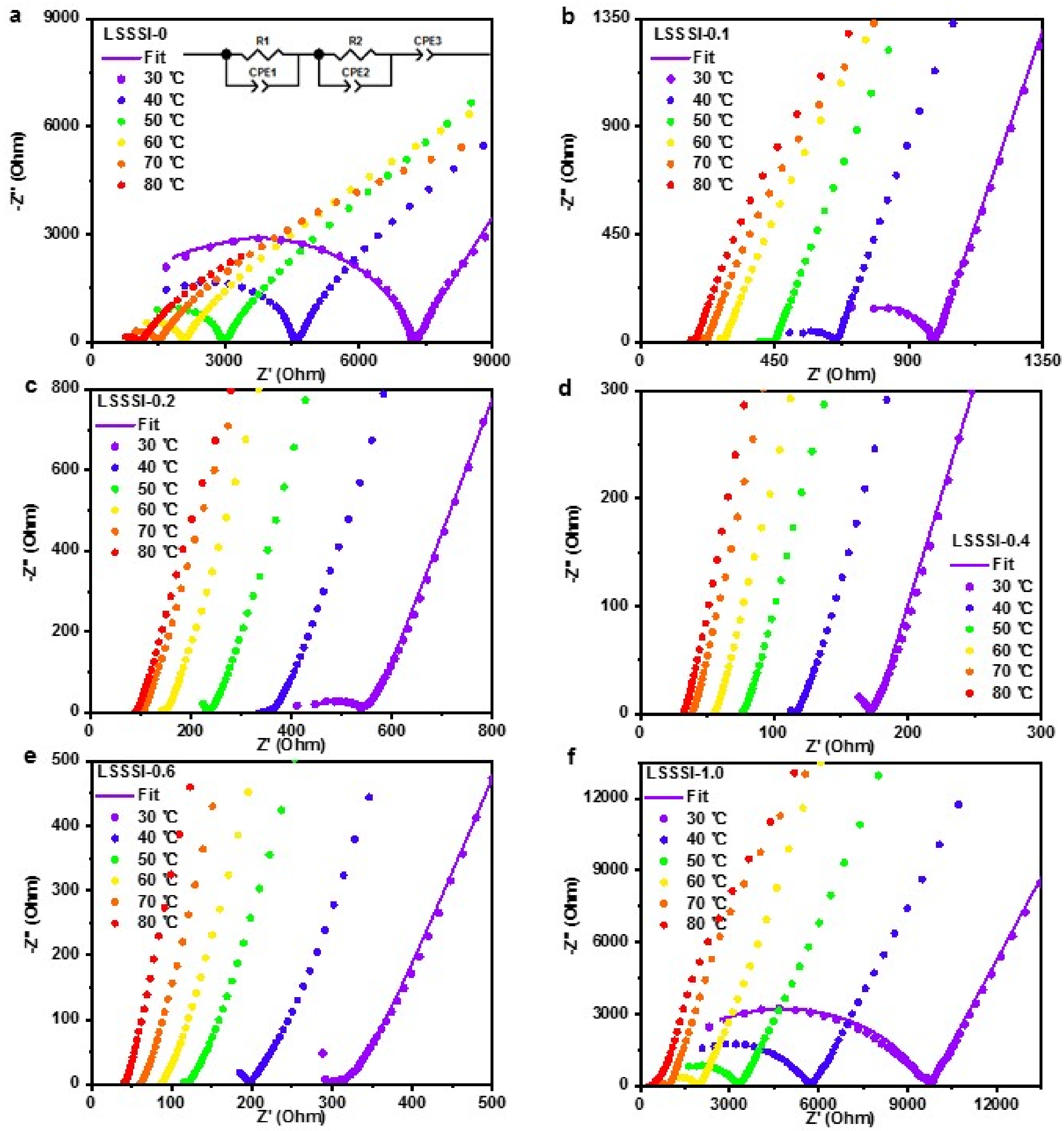

Fig. S5. Impedance spectra of LSSSI-x ($0.0 \leq x \leq 1.0$) electrolytes at different temperatures from 30 to 80 °C, the inset is the corresponding equivalent circuit.

The ionic conductivity can be obtained as follows,[4]

$$\sigma = \frac{R}{LS} \qquad (1)$$

where σ is the ionic conductivity, R is the total resistance of SSEs, L is the sample thickness, S is the area of the sample.

The activation energy is calculated by[5]

$$\sigma = A\exp\left(\frac{E_a}{RT}\right) \qquad (2)$$

where A is the pre-exponential factor, E_a is the activation energy, R is the gas constant, T is the absolute temperature.

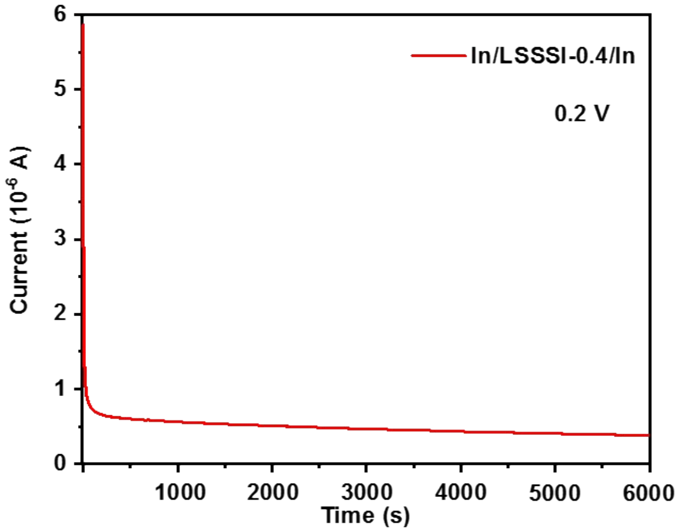

Fig. S6. DC polarization profiles of ion-blocking In/LSSSI-0.4/In cell at 0.2 V.

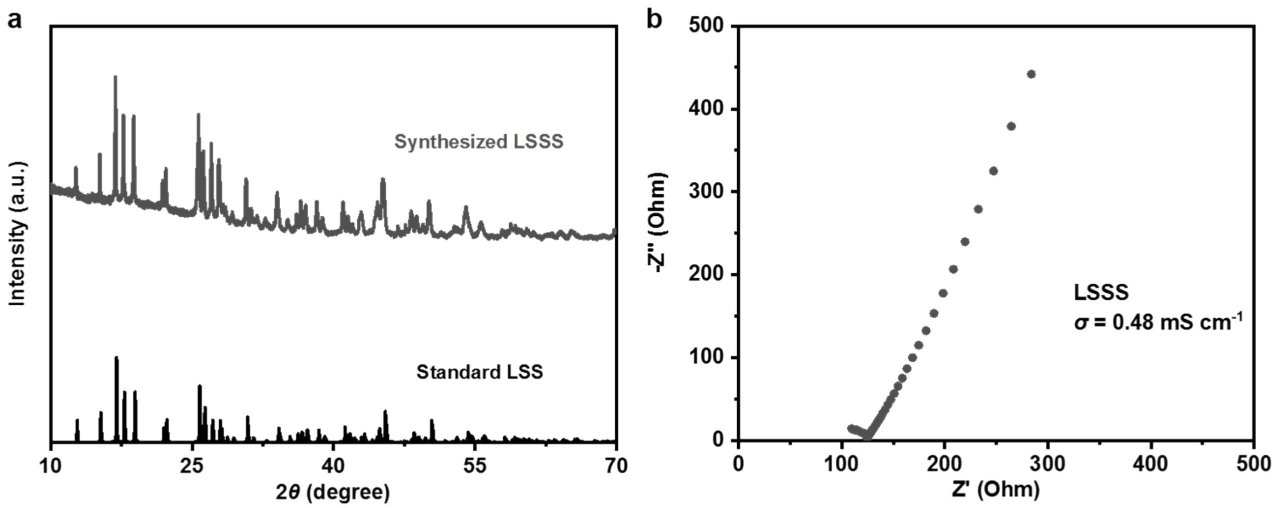

Fig. S7. (a) XRD pattern of prepared LSSS electrolyte. (b) Nyquist plot for LSSS electrolyte at 30 °C.

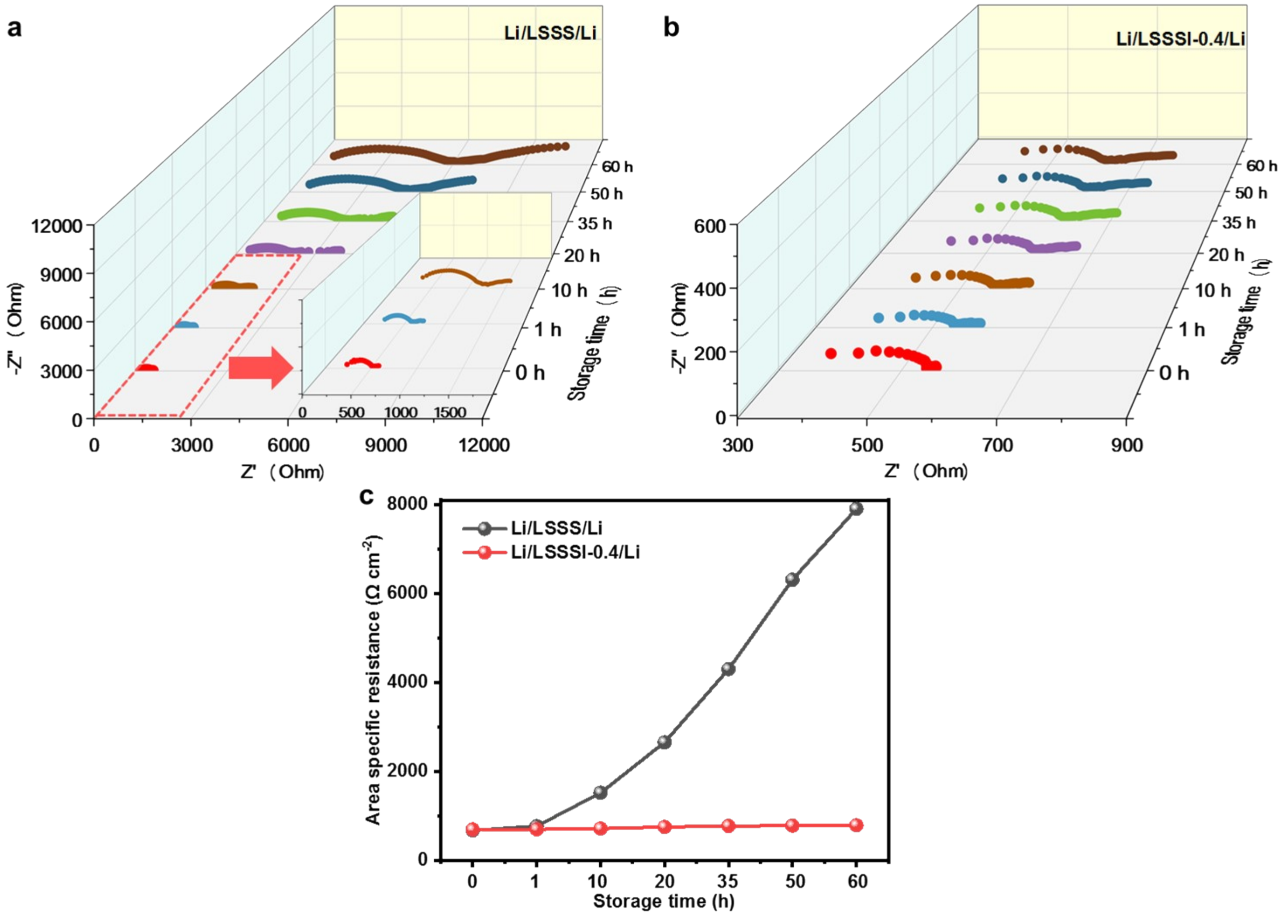

Fig. S8. Storage time dependence of EIS spectra at room temperature for (a) LSSS and (b) LSSSI-0.4, respectively. (c) The area specific resistance of Li/LSSS/Li and Li/LSSSI-0.4/Li cells as a function of storage time.

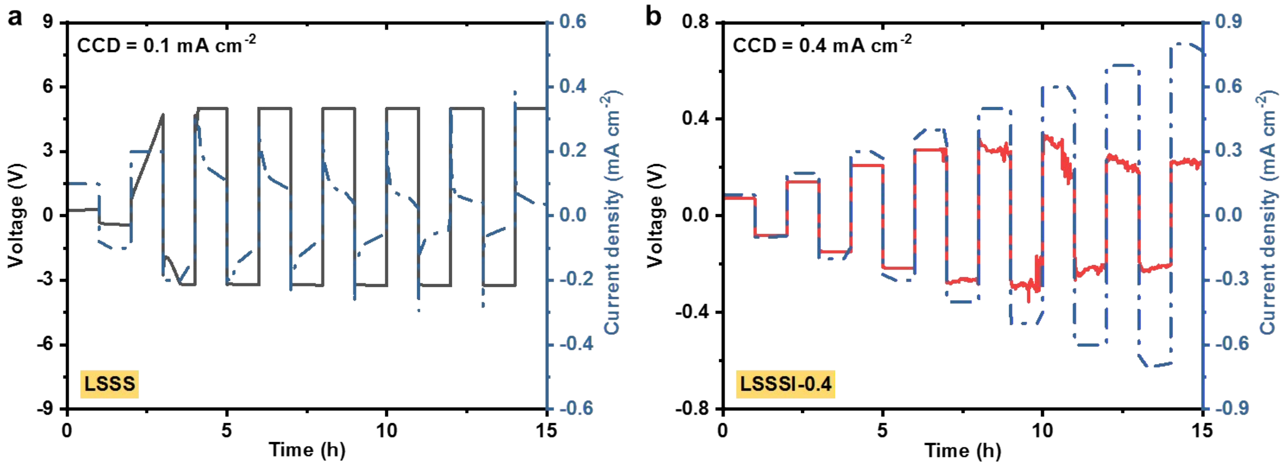

Fig. S9. Galvanostatic cycling of the Li symmetric cell at step-increased current densities of (a) Li/LSSS/Li and (b) Li/LSSSI-0.4/Li symmetric cells.

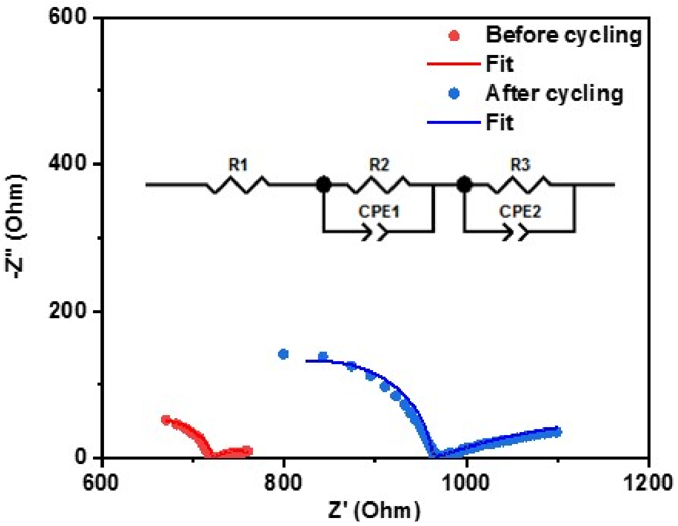

Fig. S10. The interfacial resistances of the Li/LSSSI-0.4/Li symmetric cell before and after cycling for 450 h, the inset is the corresponding equivalent circuit.

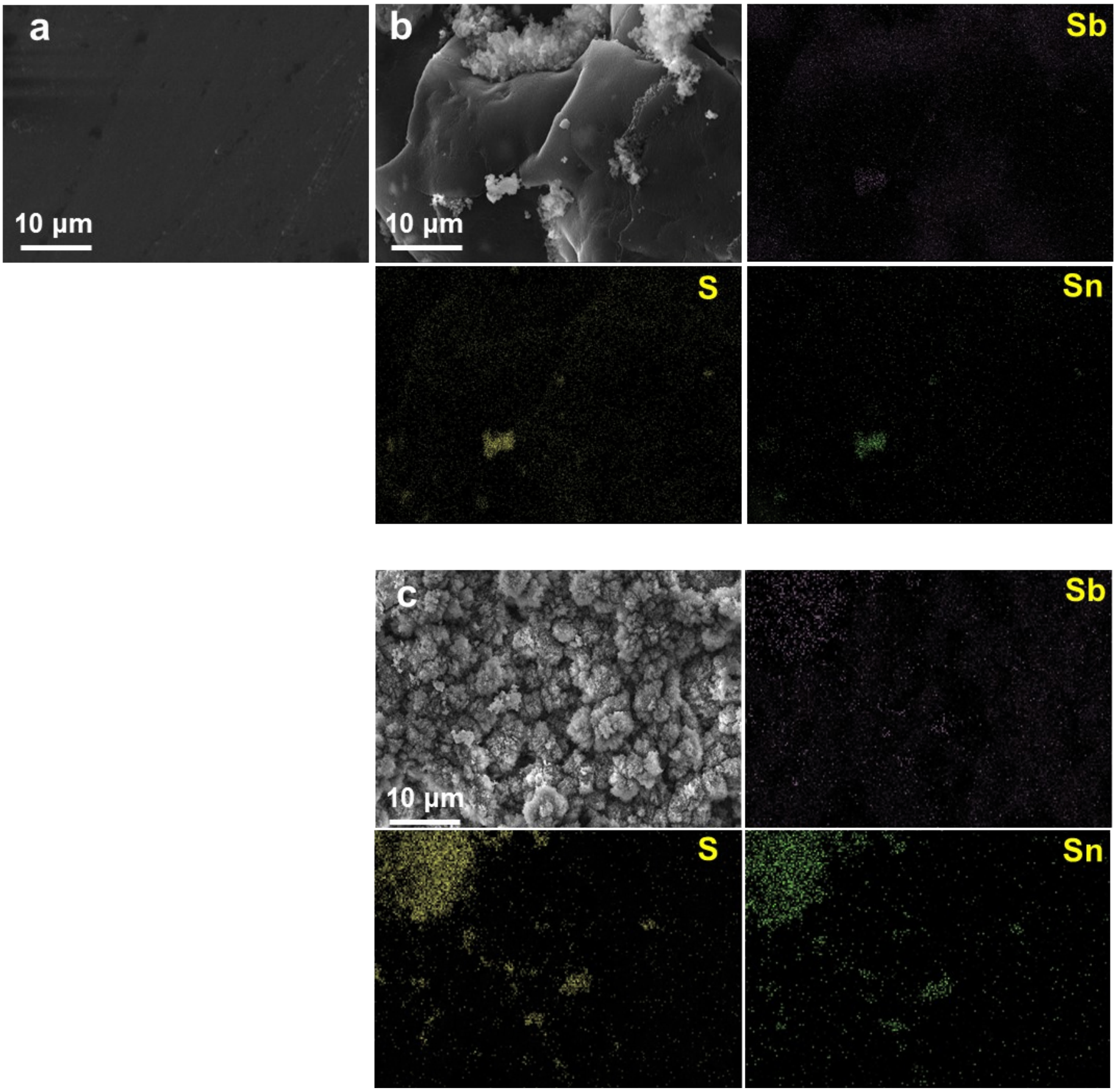

Fig. S11. (a) The morphology of the pristine Li metal. SEM images and corresponding EDS element mappings of the Li surface (b) after storage of 60 h in the Li/LSSS/Li cell and (c) after cycling at a current density of 0.1 mA cm^{-2} for 36 h.

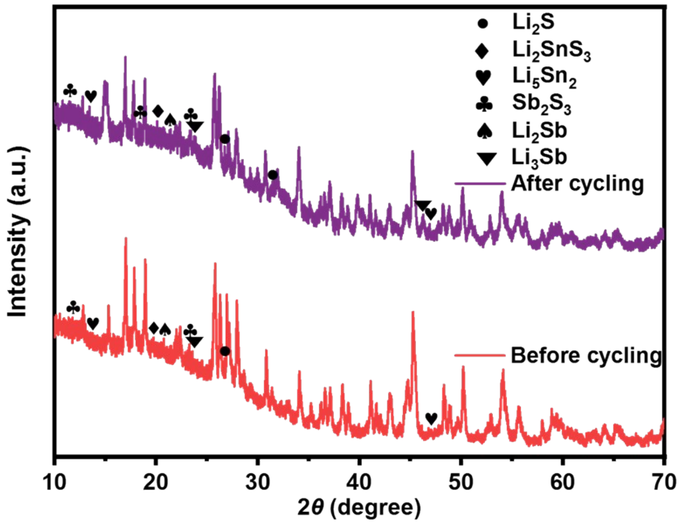

Fig. S12. XRD patterns of the interfacial compositions at Li/SSEs interfaces after 60 h of storage and 36 h cycling in the Li/LSSS/Li symmetric cell.

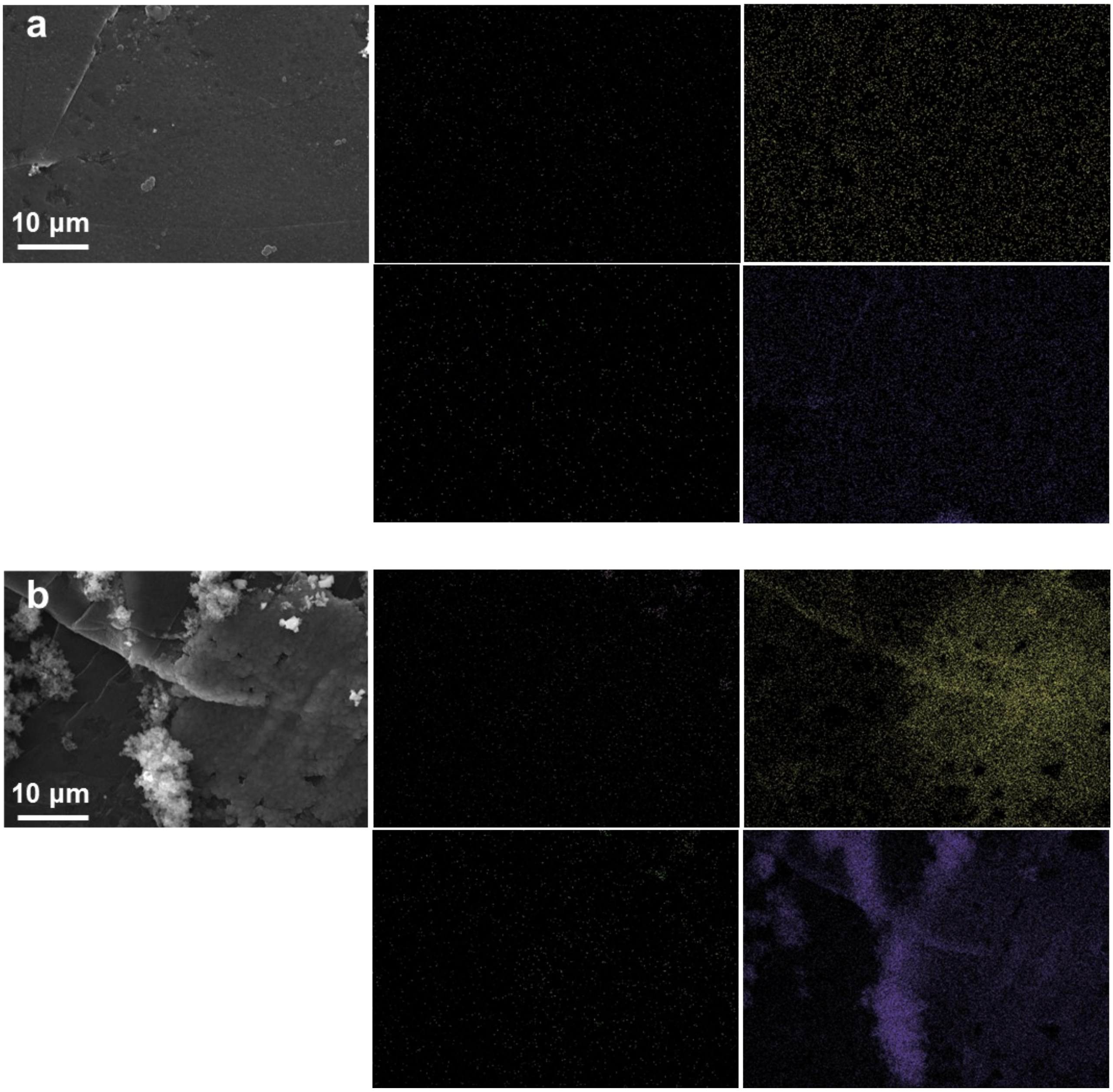

Fig. S13. SEM images and corresponding EDS element mappings of the Li surface (a) after storage of 60 h in the Li/LSSSI-0.4/Li cell and (b) after cycling at a current density of 0.1 mA cm^{-2} for 36 h.

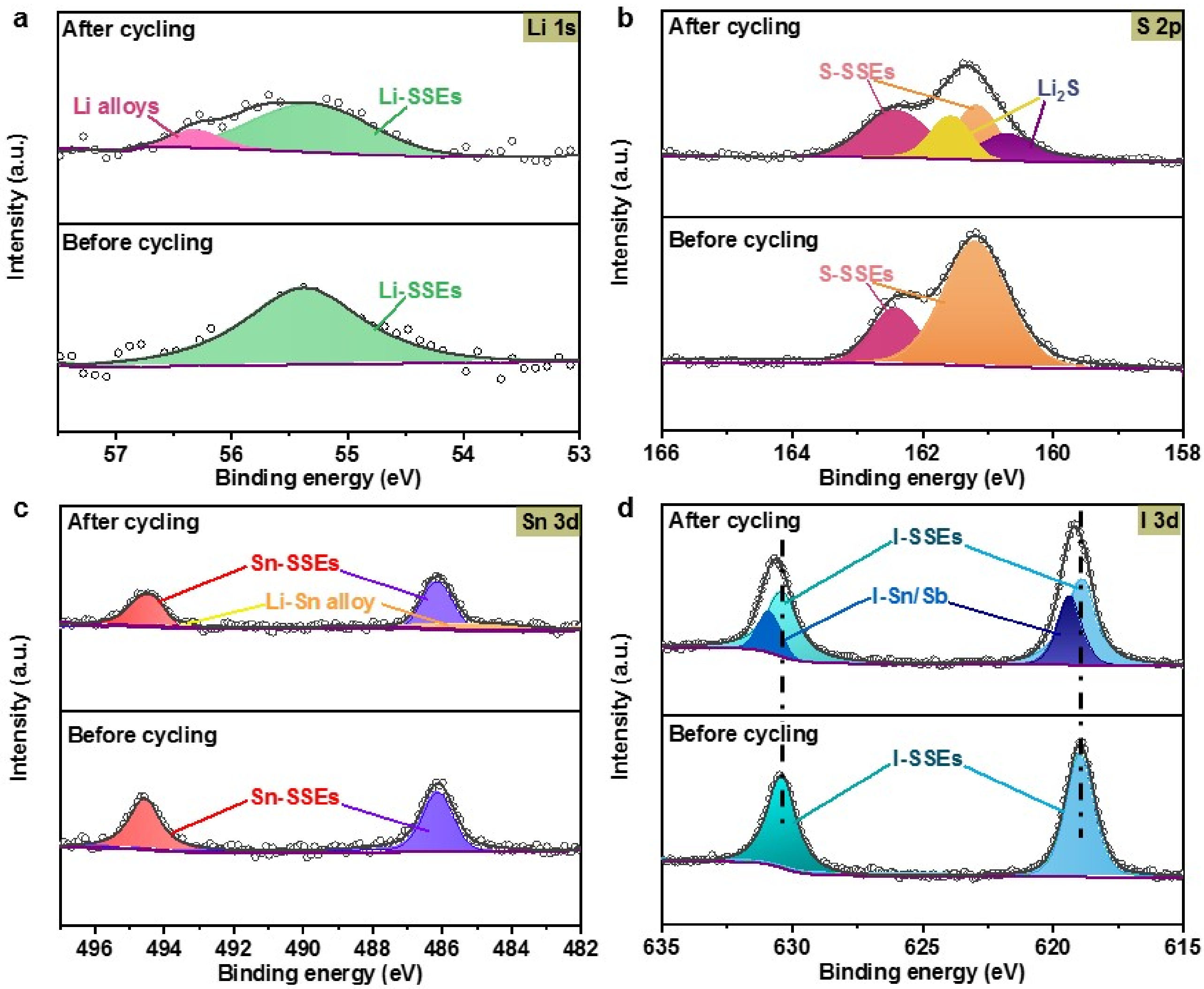

Fig. S14. (a) Li 1s, (b) S 2p, (c) Sn 3d and (d) I 3d XPS spectra of the interfacial compositions at Li/SSEs interface before and after cycling.

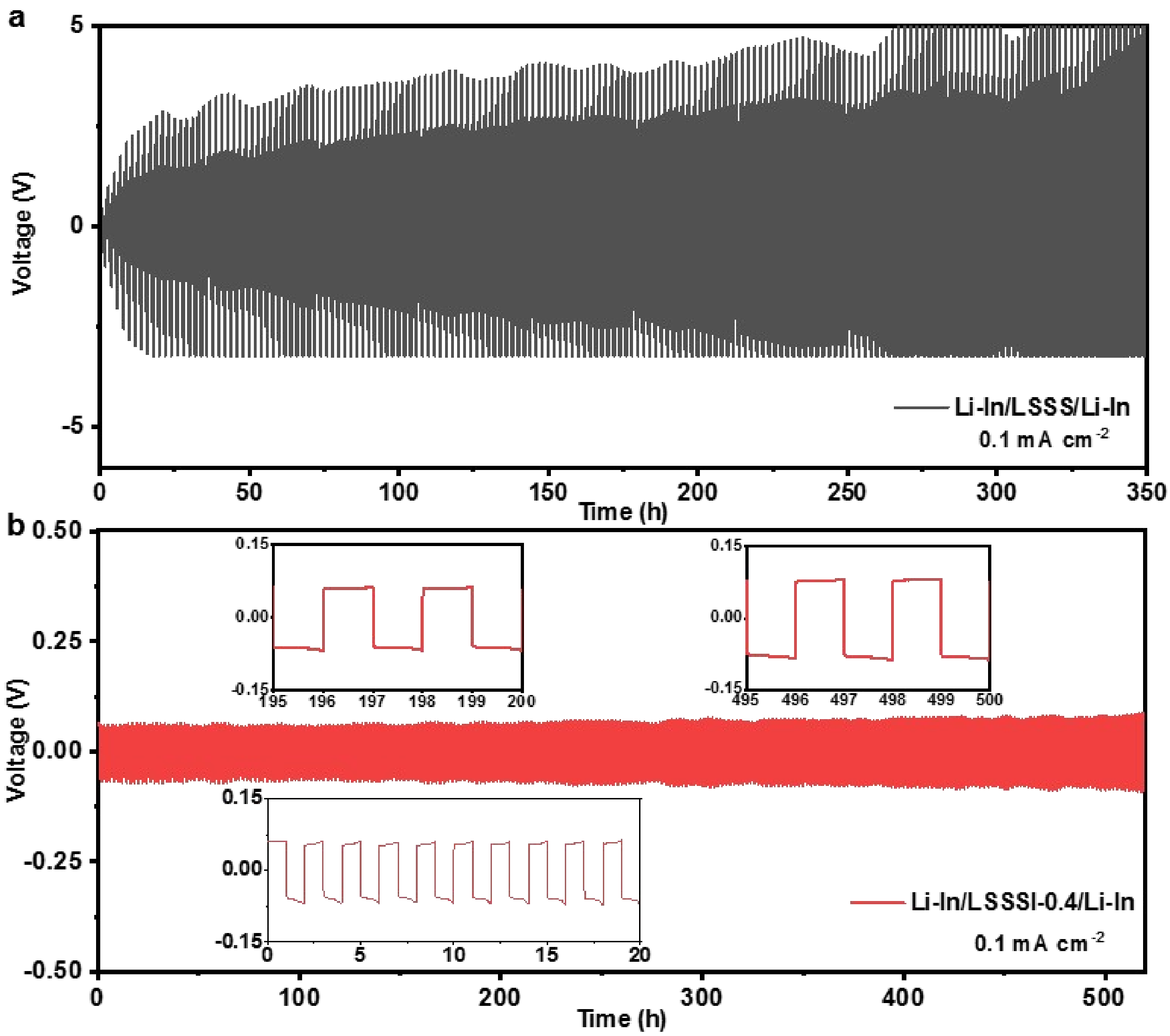

Fig. S15. Voltage profiles as a function of time during galvanostatic Li plating/stripping for (a) Li-In/LSSS/Li-In symmetric cell and (b) Li/LSSSI-0/Li symmetric cell at a current density of 0.1 mA cm^{-2}.

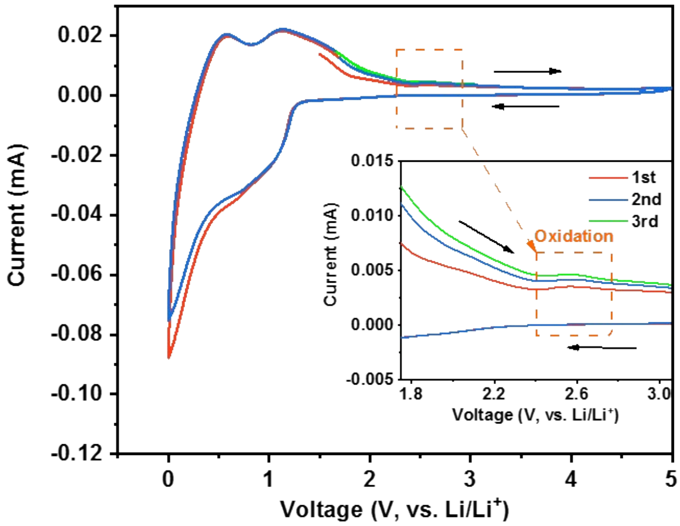

Fig. S16. The Cyclic Voltammetry of LSSSI-0.4 from 0 to 5 V *vs.* Li/Li^{+}.

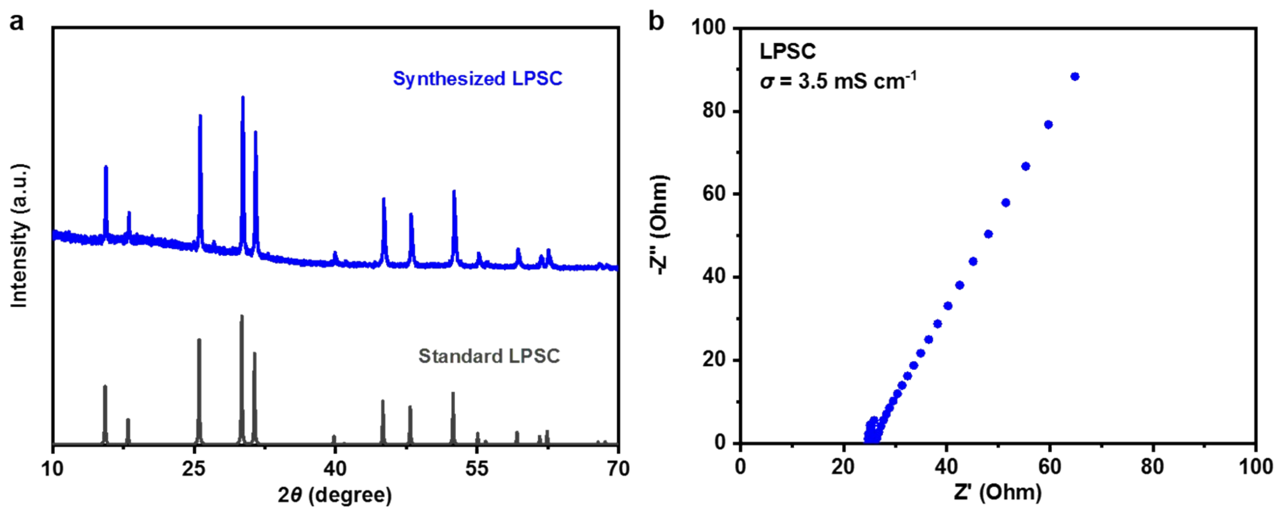

Fig. S17. (a) XRD pattern and (b) Nyquist plot of prepared LPSC electrolyte at room temperature.

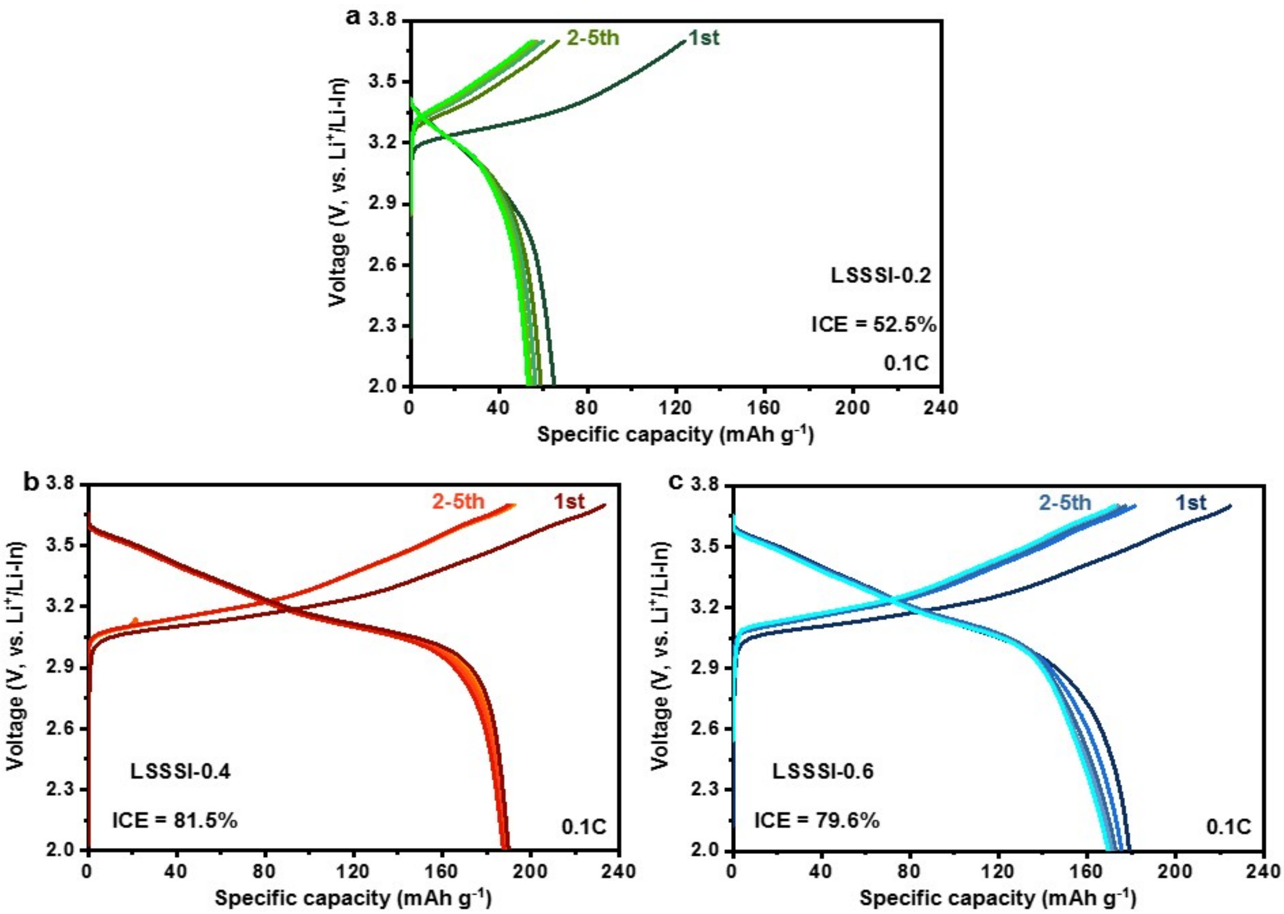

Fig. S18. Galvanostatic charge and discharge curves of the optimized ASSLBs using (a) LSSSI-0.2, (b) LSSSI-0.4 and (c) LSSSI-0.6 electrolytes at 0.1C.

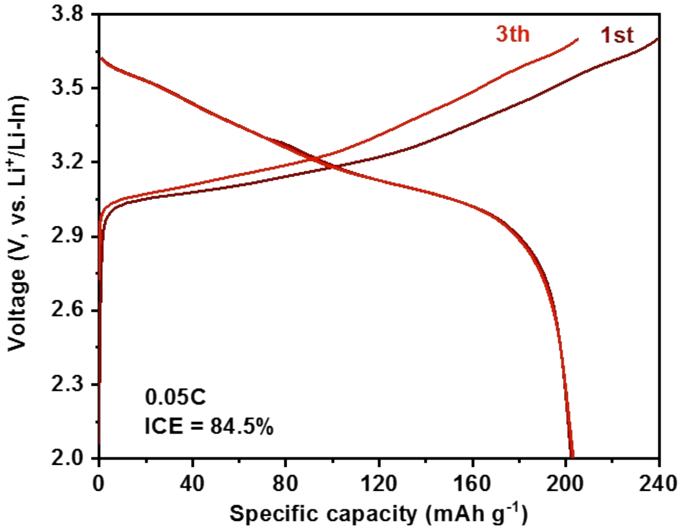

Fig. S19. Charge-discharge curves of the optimized ASSLB from 2.0 to 3.7 V (*vs.* Li^+/Li-In) at 0.05C.

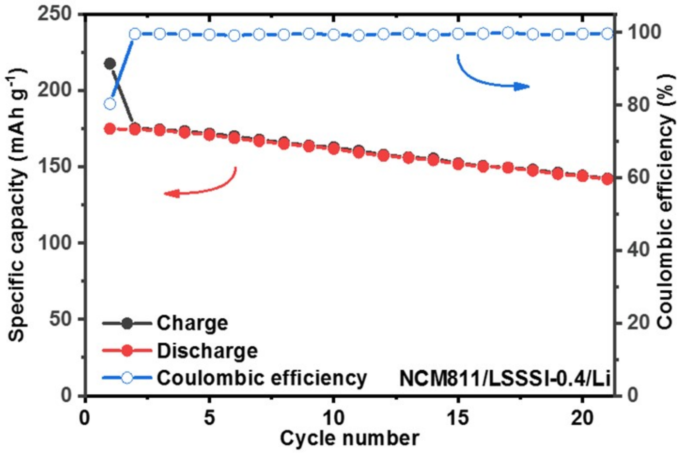

Fig. S20. The cycling performance of ASSLMB at 0.05C.

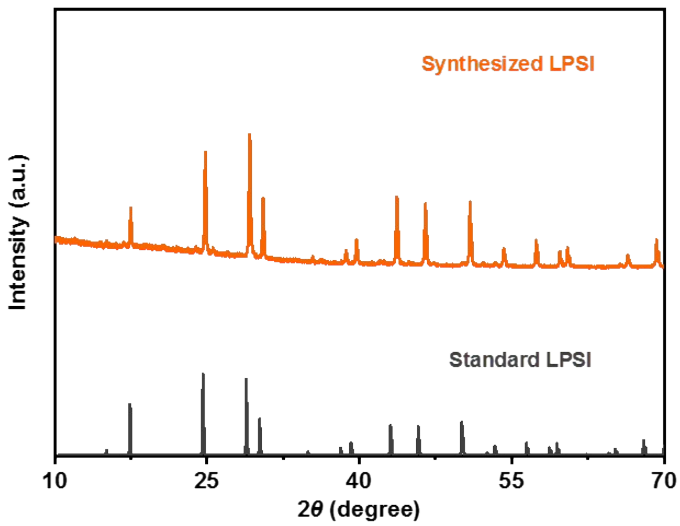

Fig. S21. XRD pattern of synthesized LPSI electrolyte.

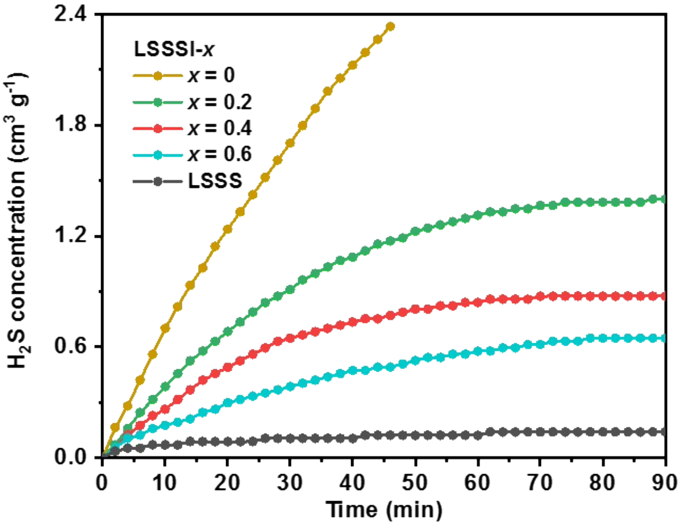

Fig. S22. Amount of H_2S gas generated when LSSSI-*x* ($0.0 \leq x \leq 0.6$) and LSSS powders were exposed to humid air.

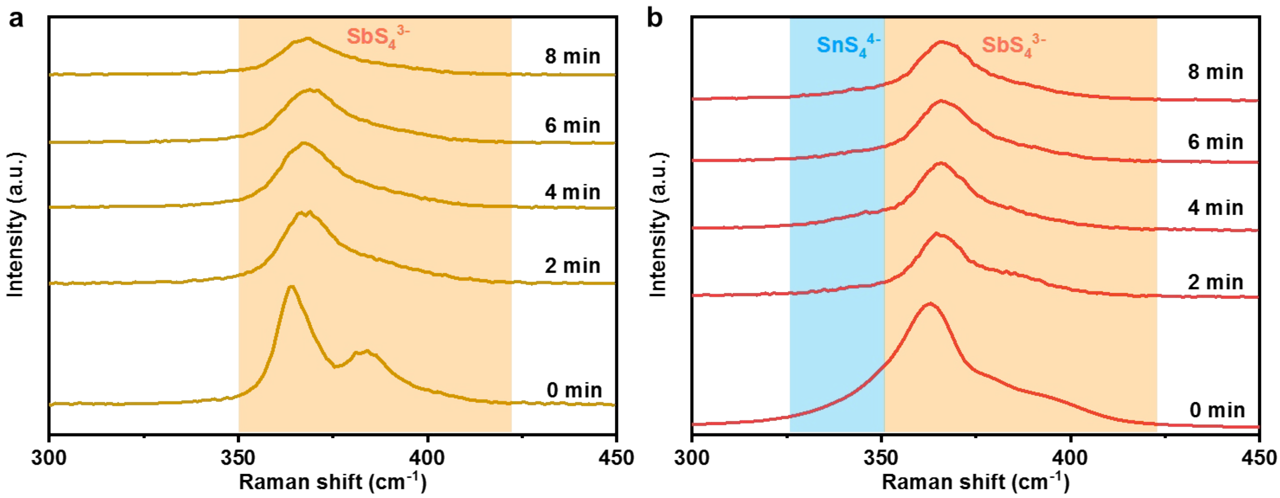

Fig. S23. In-situ Raman spectra of (a) LSSSI-0 and (b) LSSSI-0.4 after exposure to humid air (~71% RH, 26 °C).

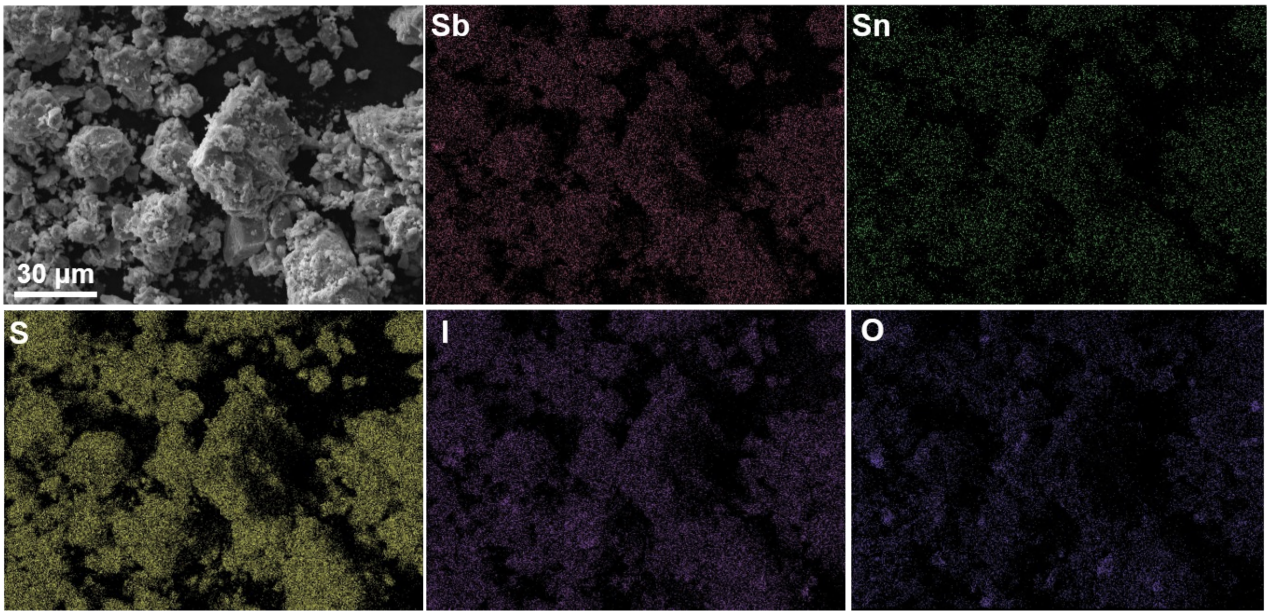

Fig. S24. SEM and corresponding EDS elemental mapping images of dried LSSSI-0.4 electrolyte.

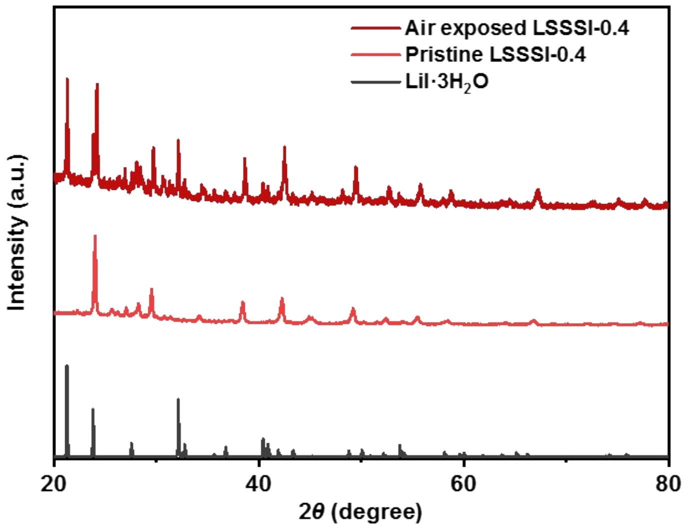

Fig. S25. XRD patterns of the as-synthesized LSSSI-0.4 and air exposed LSSSI-0.4 electrolytes.

Table S1. XRD Rietveld refinement results of LSSSI-0 with space group *F*4*m*.

a = 10.43676Å, R_p = 4.89%, R_{wp} = 6.87%					
Atom	Wyckoff site	x	y	z	Occupancy
Sb1	4b	0.5	0.5	0.5	1
S1	4c	0.25	0.25	0.25	1
S2	16e	0.37253	0.37253	0.62777	1
I1	4a	0.5	0.5	0	1
Li1	48h	0.28167	0.53204	0.78237	0.5

Table S2. XRD Rietveld refinement results of LSSSI-0.2 with space group *F*4*m*.

a = 10.45685Å; R_p = 5.23%; R_{wp} = 6.88%; 5.28 wt% LSS, 2.24 wt% Li_2S					
Atom	Wyckoff site	x	y	z	Occupancy
Sb1	4b	0.5	0.5	0.5	0.808
Sn1	4b	0.5	0.5	0.5	0.192
S1	4c	0.25	0.25	0.25	0.952
S2	16e	0.37203	0.37203	0.62866	1
I1	4a	0.5	0.5	0	1
I2	4c	0.25	0.25	0.25	0.048
Li1	48h	0.28322	0.53192	0.78022	0.516

Table S3. XRD Rietveld refinement results of LSSSI-0.4 with space group *F*4*m*.

a = 10.46601Å; R_p = 5.55%; R_{wp} = 7.46%; 17.06 wt% LSS, 4.35 wt% Li_2S, 0.73 wt% LiI

Atom	Wyckoff site	x	y	z	Occupancy
Sb1	4b	0.5	0.5	0.5	0.616
Sn1	4b	0.5	0.5	0.5	0.384
S1	4c	0.25	0.25	0.25	0.952
S2	16e	0.37169	0.37169	0.62915	1
I1	4a	0.5	0.5	0	1
I2	4c	0.25	0.25	0.25	0.048
Li1	48h	0.28480	0.53280	0.79200	0.533

Table S4. XRD Rietveld refinement results of LSSSI-0.6 with space group *F*4*m*.

a = 10.48021Å; R_p = 6.18%; R_{wp} = 8.37%; 36.30 wt% LSS, 7.38 wt% Li_2S, 3.04 wt% LiI, 0.09 wt% Sn_4SI_6

Atom	Wyckoff site	x	y	z	Occupancy
Sb1	4b	0.5	0.5	0.5	0.432
Sn1	4b	0.5	0.5	0.5	0.568
S1	4c	0.25	0.25	0.25	0.952
S2	16e	0.37057	0.37057	0.63036	1
I1	4a	0.5	0.5	0	1
I2	4c	0.25	0.25	0.25	0.048
Li1	48h	0.28631	0.53378	0.77723	0.550

Table S5. Ionic conductivities and activation energies of sulfide solid state electrolytes.

Composition	Conductivity [S cm^{-1}]	E_a [eV]	Ref.
$Li_{9.54}Si_{1.74}P_{1.44}S_{11.7}Cl_{0.3}$	2.5×10^{-2}	0.24	[6]
$Li_{9.54}[Si_{0.6}Ge_{0.4}]_{1.74}P_{1.44}S_{11.1}Br_{0.3}O_{0.6}$	3.2×10^{-2}	0.24	[7]
Li_6PS_5I	2.8×10^{-6}	0.42	[8]
$Li_{6.2}Sn_{0.2}P_{0.8}S_5I$	3.5×10^{-4}	0.30	[8]
Li_6PS_5Cl	2.4×10^{-3}	0.32	[9]
Li_4SnS_4	7.0×10^{-5}	0.41	[10]
$Li_{3.875}Sn_{0.875}As_{0.125}S_4$	1.5×10^{-3}	0.27	[11]
$Li_{3.85}Sn_{0.85}Sb_{0.15}S_4$	4.6×10^{-4}	0.50	[12]
Li_6SbS_5I	3.0×10^{-6}	0.38	[3]
$Li_{6.5}Ge_{0.5}Sb_{0.5}S_5I$	1.61×10^{-2}	0.18	[3]
$Li_{6.7}Si_{0.7}Sb_{0.3}S_5I$	1.12×10^{-2}	0.26	[13]
LSSSI-0.4	3.49×10^{-4}	0.31	This work

Table S6. The comparison of electrochemical properties of this work with other published ASSLBs based on air-exposed SSEs.

Assembled batteries	Voltage (V *vs.* Li/Li$^+$)	Loading mass (mg cm^{-2})	Initial discharge capacity (mAh g^{-1})	Cycle life	Reference
NCM811/LSSSI-0.4/Li-In	2.6~4.3	8.92	184.0 (0.1C, 30 °C) 131.7 (0.2C, 30 °C)	>600	This work
0.4LiI-0.6Li_4SnS_4@$LiCoO_2$/Li_3PS_4/Li-In	3.0~4.3	16.23	~118 (0.1C, 30 °C)	-	[14]
Li_4SnS_4@$LiCoO_2$/$Li_{10}GeP_2S_{12}$/Li_3PS_4/Li-In	3.0~4.3	16.23	~110 (0.1C, 30 °C)	30	[15]
$LiCoO_2$/$Li_{10}Ge(P_{0.925}Sb_{0.075})_2S_{12}$/In	2.5~4.2	8.92	126.0 (0.1C, RT)	>50	[16]
$LiCoO_2$/$Li_{3.875}Sn_{0.875}As_{0.125}S_4$/$Li_4Ti_5O_{12}$	0.6~3.2	1.27	188.4 (0.1C, 30 °C)	210	[11]
NCM811/$Li_{9.54}Si_{1.74}(P_{9.903}Sb_{0.097})_2S_{11.7}Cl_{0.3}$/graphite/Li	2.5~4.3	2.0	182.4 (0.5C, 55 °C)	30	[17]
NCM622/$Li_{6.04}P_{0.98}Bi_{0.02}S_{4.97}O_{0.03}Cl$/Li	2.5~4.3	8.79	~120.0 (0.2C, RT)	40	[18]

where RT stands for room temperature.

References:

1 T. J. Whittles, T. D. Veal, C. N. Savory, A. W. Welch, J. T. Gibbon, M. Birkett, R. J. Potter, D. O. Scanlon, A. Zakutayev and V. R. Dhanak, *ACS Appl. Mater. Interfaces*, 2017, **9**, 41916.

2 N. Fleck, O. S. Hutter, L. J. Phillips, H. Shiel, T. D. Hobson, V. R. Dhanak, T. D. Veal, F. Jäckel, K. Durose and J. D. Major, *ACS Appl. Mater. Interfaces*, 2020, **12**, 52595.

3 Y. Lee, J. Jeong, H. J. Lee, M. Kim, D. Han, H. Kim, J. M. Yuk, K.-W. Nam, K. Y. Chung, H.-G. Jung and S. Yu, *ACS Energy Lett.*, 2022, **7**, 171.

4 M. B. Preefer, J. H. Grebenkemper, F. Schroeder, J. D. Bocarsly, K. Pilar, J. A. Cooley, W. Zhang, J. Hu, S. Misra, F. Seeler, K. Schierle-Arndt and R. Seshadri, *ACS Appl. Mater. Interfaces*, 2019, **11**, 42280.

5 G. Liu, D. Xie, X. Wang, X. Yao, S. Chen, R. Xiao, H. Li and X. Xu, *Energy Storage Mater.*, 2019, **17**, 266.

6 Y. Kato, S. Hori, T. Saito, K. Suzuki, M. Hirayama, A. Mitsui, M. Yonemura, H. Iba and R. Kanno, *Nat. Energy*, 2016, **1**, 16030.

7 Y. Li, S. Song, H. Kim, K. Nomoto, H. Kim, X. Sun, S. Hori, K. Suzuki, N. Matsui, M. Hirayama, T. Mizoguchi, T. Saito, T. Kamiyama and R. Kanno, *Science*, 2023, **381**, 50.

8 F. Zhao, J. Liang, C. Yu, Q. Sun, X. Li, K. Adair, C. Wang, Y. Zhao, S. Zhang, W. Li, S. Deng, R. Li, Y. Huang, H. Huang, L. Zhang, S. Zhao, S. Lu and X. Sun, *Adv. Energy Mater.*, 2020, **10**, 1903422.

9 H. Liu, Q. Zhu, Y. Liang, C. Wang, D. Li, X. Zhao, L. Gao and L.-Z. Fan, *Chem. Eng. J.*, 2023, **462**, 142183.

10 T. Kaib, S. Haddapour, M. Kapitein, P. Bron, C. Schröder, H. Eckert, B. Roling and S. Dehnen, *Chem. Mater.,* 2012, **24**, 2211.

11 P. Lu, L. Liu, S. Wang, J. Xu, J. Peng, W. Yan, Q. Wang, H. Li, L. Chen and F. Wu, *Adv. Mater.*, 2021, **33**, 2100921.

12 H. Kwak, K. H. Park, D. Han, K.-W. Nam, H. Kim and Y. S. Jung, *J. Power Sources*, 2020,

446, 227338.

13 L. Zhou, A. Assoud, Q. Zhang, X. Wu and L. F. Nazar, *J. Am. Chem. Soc.*, 2019, **141**, 19002.

14 K. H. Park, D. Y. Oh, Y. E. Choi, Y. J. Nam, L. Han, J.-Y. Kim, H. Xin, F. Lin, S. M. Oh and Y. S. Jung, *Adv. Mater.*, 2016, **18**, 1874.

15 Y. E. Choi, K. H. Park, D. H. Kim, D. Y. Oh, H. R. Kwak, Y.-G. Lee and Y. S. Jung, *ChemSusChem*, 2017, **10**, 2605.

16 J. Liang, N. Chen, X. Li, X. Li, K. R. Adair, J. Li, C. Wang, C. Yu, M. N. Banis, L. Zhang, S. Zhao, S. Lu, H. Huang, R. Li, Y. Huang and X. Sun, *Chem. Mater.*, 2020, **32**, 2664.

17 L. Ye, E. Gil-González and X. Li, *Electrochem. Commun.*, 2021, **128**, 107058.

18 H. Liu, Q. Zhu, C. Wang, G. Wang, Y. Liang, D. Li, L. Gao and L.-Z. Fan, *Adv. Funct. Mater.*, 2022, **32**, 2203858.